Fracture analysis of cracked thermopiezoelectric materials by BEM

Qing-Hua Qin
Department of Mechanics, Tianjin University, Tianjin, 300072, P.R. China
E-Mail: Qhqin@tju.edu.cn

Abstract

The boundary element formulation for analysing cracked thermopiezoelectric materials due to thermal and electroelastic loads is reviewed in this paper. By way of Green's functions for piezoelectric solid with defects and variational principle, a boundary element model (BEM) for a 2-D thermopiezoelectric solid with various defects is discussed. The method is applicable to multiple crack problems in both finite and infinite solids. Finally a brief assessment of the boundary element formulation is made by considering some numerical examples for stress and electric displacement (SED) intensity factors at a particular crack-tip in a crack system of piezoelectric materials.

1 Introduction

Thermoelectroelastic analysis of multiple cracks inside a piezoelectric solid is of considerable importance in the field of fracture mechanics, as the piezoelectric materials often contains many internal microcracks before in use. Analytical analysis of thermopiezoelectric solid with defects is, however, very difficult due to its complex geometry and mathematical formulation. Thus efficient numerical techniques such as boundary element method is required to develop. In 1994, Lee and Jiang [1] derived a boundary integral equation of piezoelectric media by the method of weighted residuals and also obtained the fundamental solution for plane piezoelectricity by using the double Fourier transform technology. Lu and Mahrenholtz [2] presented a variational boundary integral equation for the same problem. Ding *et al*. [3] developed a boundary integral formulation which is efficient for analysing crack problems in piezoelectric material. Rajapakse [4] discussed three boundary element methods (direct boundary method, indirect boundary element method and fictitious stress-electric charge method) in coupled electroelastic problems. Xu and Rajapakse [5] extended the formulations to the case of piezoelectric solids with various defects (cavities, inclusions, cracks, etc.). Using Radom transform techniques, Hill and Farris [6] expressed a foundational solution for three-dimensional piezoelectric materials in a line integral form which can be evaluated numerically. Khutoryaansky *et al*. [7] introduced a boundary element formulation for time-dependent problems of linear piezoelectricity. Recently, Qin [8] and Qin and Lu [9] proposed a boundary element formulation for fracture analysis of thermopiezoelectricity based on the dislocation method and the potential variational principle. Liu and Hui[10] presented a boundary integral equation for analyzing thin piezoelectric films and coatings. The following developments are based on Qin[8,11], Qin and Lu[9], and Qin and Mai[12].

2 Basic formulations for thermopiezoelectricity

Consider a linear piezoelectric solid in which all fields are assumed to depend only on in-plane coordinates x_1 and x_2. Boldfaced symbols stand for either column vectors or matrices, depending on whether lower case or upper case is used. The SED vector Π_i, The elastic displacement and electric potential (EDEP) vector **u**, temperature T and heat flux h_i in the solid subjected to loading can be expressed in terms of complex analytic functions as follows[11]:

$$\begin{aligned}
&T = g'(z_t) + \overline{g'(z_t)},\ \ \vartheta = -ikg'(z_t) + ik\overline{g'(z_t)},\ \ h_1 = -\vartheta_{,2},\ \ h_2 = \vartheta_{,1},\\
&\mathbf{u} = \mathbf{AF(z)q} + \mathbf{c}g(z_t) + \overline{\mathbf{AF(z)q}} + \overline{\mathbf{c}g(z_t)},\\
&\phi = \mathbf{BF(z)q} + \mathbf{d}g(z_t) + \overline{\mathbf{BF(z)q}} + \overline{\mathbf{d}g(z_t)},\\
&\Pi_1 = -\phi_{,2},\ \ \Pi_2 = \phi_{,1}
\end{aligned} \tag{1}$$

with

$$\mathbf{F(z)} = \mathrm{diag}[f(z_1)\ f(z_2) f(z_3)\ f(z_4)],\ \ z_t = x_1 + \tau x_2,\ z_i = x_1 + p_i x_2 \tag{2}$$

where overbar denotes the complex conjugate, a prime represents differentiation, **q** is a constant vector to be determined by boundary conditions, $\mathbf{u}=\{u_1\ u_2\ u_3\ \varphi\}^T$, $\mathbf{\Pi}_j=\{\sigma_{1j}\ \sigma_{2j}\ \sigma_{3j}\ D_j\}^T$, j=1,2; $i=\sqrt{-1}$, $k=\sqrt{k_{11}k_{22}-k_{12}^2}$, k_{ij} are the coefficients of heat conduction, u_i and φ are the elastic displacement and electric potential, T, h_i, σ_{ij} and D_i are temperature, heat flux, stress and electric displacement, ϑ is the heat flow function, τ and p_i are the heat and electroelastic eigenvalues of the materials whose imaginary parts are positive, $f(z_i)$ and $g(z_t)$ are arbitrary functions with complex arguments z_i and z_t, respectively, **A** , **B**, **c** and **d** are well-defined in the literature (see[11], for example).

3 BEM for thermopiezoelectric problem

Consider a two-dimensional thermoelectroelastic solid inside of which there are a number of cracks. The numerical approach to such a thermoelectroelastic problem will involve two steps: (1) solve a heat transfer problem first to obtain the steady-state T field; (2) calculate the SED caused by the T field, then derive an isothermal solution to satisfy the corresponding mechanical and electric boundary conditions, and finally, solve the modified problem for the EDEP and SED fields. The details are as follows.

3.1 BEM for temperature discontinuity problem

Consider a thermal finite region Ω_1 with a number of cracks bounded by Γ, as shown in Fig. 1(a). The heat transfer problem to be considered may be stated as

$$k_{ij}T_{,ij} = 0, \qquad \text{in } \Omega_1, \tag{3}$$

$$h_n = h_i n_i = h_0, \qquad \text{on } \Gamma_h, \tag{4}$$

$$T = T_0, \qquad \text{on } \Gamma_T, \tag{5}$$

$$h_i n_i = 0, \qquad \text{on } L, \tag{6}$$

where n_i is the normal to the boundary $\Gamma\ (=\Gamma_h + \Gamma_T)$, h_0 and T_0 are the prescribed values of heat flow and temperature, which act on the boundaries Γ_h and Γ_T, respectively. For simplicity, we define $\hat{T} = T\big|_{L^+} - T\big|_{L^-}$ on $L(=L^+ + L^-)$, where $\hat{T}$ is the temperature discontinuity, L is the union of all cracks, L^+ and L^- are defined in Fig. 1(b).

Further, if we let Ω_2 be the complementary region of Ω_1 (i.e., the union of Ω_1 and Ω_2 forms the infinite region Ω) and $\hat{T} = T\big|_{\Gamma^+} - T\big|_{\Gamma^-} = T_0$, Γ^+ and Γ^- are defined in Fig. 1(b), the problem shown in Fig 1(a) can be extended to the infinite case (see Fig. 1b).

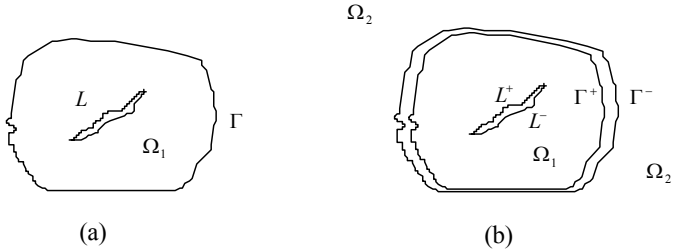

Fig. 1: Configuration of piezoelectric plate for BEM analysis.

3.1.1 Potential variational principle

In a similar manner to that of Yin and Ehrlacher [13], the total generalized potential energy for the thermal problem defined above can be given as

$$P(T,\hat{T}) = \frac{1}{2}\int_\Omega k_{ij} T_{,i} T_{,j} d\Omega + \int_\Gamma h_n \hat{T} dL\,. \tag{7}$$

By transforming the region integral in eqn (7) into a boundary integral, we have

$$P(T,\hat{T}) = -\frac{1}{2}\int_L \vartheta(T)\hat{T}_{,s} ds + \int_\Gamma h_n \hat{T} ds\,, \tag{8}$$

in which the relation

$$h_i = -k_{ij} T_{,j}, \qquad \int_L h_n \hat{T} ds = \int_L [(\vartheta\hat{T})_{,s} - \vartheta\hat{T}_{,s}] ds\,, \tag{9}$$

and the temperature discontinuity assumed to be continuous over L and being zero at the ends of L are used. Moreover, temperature T in eqn (8) can be expressed in terms of $\hat{T}$ through use of Green's function presented in [11]. Thus, the potential energy can be further written as

$$P(\hat{T}) = -\frac{1}{2}\int_L \vartheta(\hat{T})\hat{T}_{,s} ds + \int_\Gamma h_n \hat{T} ds\,. \tag{10}$$

3.1.2 Boundary element formulation

Analytical results for the minimum potential (10) are not, in general, possible, and therefore a numerical procedure must be used to solve the problem. As in the conventional BEM, the boundaries Γ and L are divided into M_Γ and M_L linear boundary elements, for which the temperature discontinuity may be approximated by the sum of elemental temperature discontinuities:

$$\hat{T}(s) = \sum_{m=1}^{M} \hat{T}_m F_m(s) \tag{11}$$

where $\hat{T}_m$ is the temperature discontinuity at node m, M= $M_\Gamma + M_L + N$, and N is the number of cracks. It should be mentioned that appearance of N is due to the number of nodes being one more than the number of element in each crack.

With the use of Green's functions presented in [11] and eqn (11), the temperature and heat-flow function at point z_t (or $\zeta_t(z_t)$ which is defined in the Appendix A) can be given as

$$T(\zeta_t) = \sum_{m=1}^{M} \mathrm{Im}[a_m(\zeta_t)]\hat{T}_m \tag{12}$$

$$\vartheta(\zeta_t) = -k\sum_{m=1}^{M} \mathrm{Re}[a_m(\zeta_t)]\hat{T}_m \tag{13}$$

where $a_m(\zeta_t)$ has different form for different problem(see Appendix A for details).

In particular the temperature at node j can be written as

$$T_j[f(d_j)] = \sum_{m=1}^{M} \mathrm{Im}\{a_m[f(d_j)]\}\hat{T}_m \,. \tag{14}$$

where $d_j = x_{1j} + p_1^* x_{2j}$, (x_{1j}, x_{2j}) are the coordinates at node j.

For the total potential energy (10), through the substitution of eqns (11) and (13) into it, one obtains

$$P(\hat{T}) \approx \sum_{j=1}^{M}\left[\sum_{m=1}^{M}\left(-\frac{1}{2}K_{mj}\hat{T}_m\hat{T}_j\right) + G_j\hat{T}_j\right] \tag{15}$$

where K_{mj} is the so-called stiffness matrix and G_j the equivalent nodal heat flow vector, with the form

$$K_{mj} = -\frac{k}{l_{j-1}}\int_{l_{j-1}} \mathrm{Re}[a_m(\zeta_{t0}^{j-1})]ds + \frac{k}{l_j}\int_{l_j} \mathrm{Re}[a_m(\zeta_{t0}^{j})]ds \,, \tag{16}$$

$$G_j = \int_{l_{j-1}+l_j} h_{*0}F_j(s)ds \,, \tag{17}$$

where $h_{*0} = h_0$ when $s \in \Gamma_h$, and $h_{*0} = 0$ for other cases.

The minimization of $P(\hat{T})$ yields

$$\sum_{j=1}^{M} K_{mj}\hat{T}_j = G_m . \tag{18}$$

The final form of linear equation to be solved is obtained by selecting the appropriate equation from eqns (14) and (18). Equation (14) will be chosen for those nodes at which the temperature is prescribed, and eqn (18) will be chosen for the remaining nodes. After the nodal temperature discontinuities have been calculated, the displacement and stress at any point in the region can be evaluated through use of eqn (1). They are

$$\mathbf{U} = \sum_{j=1}^{M} \mathbf{u}_j \hat{T}_j ,\ \boldsymbol{\Pi}_1 = \sum_{j=1}^{M} \mathbf{x}_j \hat{T}_j ,\ \boldsymbol{\Pi}_2 = \sum_{j=1}^{M} \mathbf{y}_j \hat{T}_j \tag{19}$$

where $\mathbf{u}_j$, $\mathbf{x}_j$ and $\mathbf{y}_j$ have different forms for different problems (see Appendix B for details).

3.2 BEM for displacement and potential discontinuity problems

Consider again the domain Ω_1, in which the governing equation and its boundary conditions are described as follows:

$$\boldsymbol{\Pi}_{ij,j} = 0 , \qquad \text{in } \Omega_1 , \tag{20}$$

$$t_{ni} = \Pi_{ij} n_j = t_i^0 - (\mathbf{t}_n^{\theta})_i , \qquad \text{on } \Gamma_t, \tag{21}$$

$$u_i = u_i^0 - (\mathbf{U}_T^{\theta})_i , \qquad \text{on } \Gamma_u, \tag{22}$$

$$t_{ni}\big|_{L^+} = -t_{ni}\big|_{L^-} = -(\mathbf{t}_n^{\theta})_i , \quad b_i = u_i\big|_{L^+} - u_i\big|_{L^-} - (\mathbf{U}_T^{\theta})_i\big|_{L^+} + (\mathbf{U}_T^{\theta})_i\big|_{L^-} , \quad \text{on } L \tag{23}$$

where Γ_t and Γ_u are the boundaries on which the prescribed values of stress t_i^0 and displacement u_i^0 are imposed. Similarly, the related potential energy for the elastic problem can be given as

$$P(\mathbf{b}) = \frac{1}{2}\int_L [\varphi(\mathbf{b}) \cdot \mathbf{b}_{,s} + 2\mathbf{t}_n^0 \cdot \mathbf{b}] ds - \int_{\Gamma} (\mathbf{t}^0 - \mathbf{t}_n^{\theta}) \cdot \mathbf{b} ds \tag{24}$$

where the electroelastic solutions of functions $\varphi(\mathbf{b})$ and $\mathbf{U}(\mathbf{b})$ appearing later have been defined in Chapter 4 of Ref.[11] and are also presented in Appendix C for the sake of reference.

It should be mentioned that we use the impermeable electric boundary condition on crack faces because of its much simpler mathematical treatment and the fact that the dielectric constants of a piezoelectric material are much larger than that of the environment (generally between 1000 and 3500 times larger).

As treated before, the boundaries L and Γ are divided into a series of boundary elements, for which the EDEP discontinuity may be approximated through linear interpolation as

$$\mathbf{b}(s) = \sum_{m=1}^{M} \mathbf{b}_m F_m(s) . \tag{25}$$

With the approximation (25), the EDEP and SED functions can be expressed in the form

$$\mathbf{U}(\zeta) = \sum_{m=1}^{M} \mathrm{Im}[\mathbf{A}\mathbf{D}_m(\zeta)]\mathbf{b}_m , \qquad \varphi(\zeta) = \sum_{m=1}^{M} \mathrm{Im}[\mathbf{B}\mathbf{D}_m(\zeta)]\mathbf{b}_m \tag{26}$$

where $\mathbf{D}_m$ has different forms for different problems. The function $\mathbf{D}_m$ is given in Appendix D for four typical problems.

In particular the displacement at node j is given by

$$\mathbf{U}[\langle f(d_{\alpha j})\rangle] = \sum_{m=1}^{M} \mathrm{Im}\{\mathbf{A}\mathbf{D}_m[\langle f(d_{\alpha j})\rangle]\}\mathbf{b}_m . \tag{27}$$

Substituting eqns (25) and (26) into eqn (24), we have

$$P(\mathbf{b}) = \sum_{i=1}^{M} \left[\mathbf{b}_i^T \cdot \left(\sum_{j=1}^{M} \mathbf{k}_{ij}\mathbf{b}_j \right) / 2 - \mathbf{g}_i \right] \tag{28}$$

where

$$\mathbf{k}_{ij} = \frac{1}{l_{j-1}} \int_{l_{j-1}} \mathrm{Im}[\mathbf{D}_i^T(\boldsymbol{\zeta}_0^{j-1})\mathbf{B}^T]ds - \frac{1}{l_j} \int_{l_j} \mathrm{Im}[\mathbf{D}_i^T(\boldsymbol{\zeta}_0^{j})\mathbf{B}^T]ds \tag{29}$$

$$\mathbf{g}_j = \int_{l_{j-1}+l_j} \mathbf{G}_j F_j(s) ds \tag{30}$$

and $\mathbf{G}_j = -\mathbf{t}_n^{\theta}$ when node j is located at the boundary L, $\mathbf{G}_j = \mathbf{t}^0 - \mathbf{t}_n^{\theta}$ for the other nodes. The minimization of eqn (28) leads to a set of linear equations:

$$\sum_{j=1}^{M} \mathbf{k}_{ij}\mathbf{b}_j = \mathbf{g}_i . \tag{31}$$

Similarly, the final form of the linear equations to be solved is obtained by selecting the appropriate equation, from eqns (27) and (31). Equation (27) will be chosen for those nodes at which the EDEP is prescribed, and eqn (31) will be chosen for the remaining nodes. Once the EDEP discontinuity $\mathbf{b}$ has been found, the SED at any point can be expressed as

$$\boldsymbol{\Pi}_1 = -\sum_{m=1}^{M} \mathrm{Im}[\mathbf{B}\mathbf{P}\mathbf{D}'_m(\boldsymbol{\zeta})]\mathbf{b}_m , \quad \boldsymbol{\Pi}_2 = \sum_{m=1}^{M} \mathrm{Im}[\mathbf{B}\mathbf{D}'_m(\boldsymbol{\zeta})]\mathbf{b}_m . \tag{32}$$

Therefore, the surface traction-charge vector $\boldsymbol{\Pi}_n$ in a coordinate system local to a particular crack line, say the ith crack, can be expressed in the form

$$\boldsymbol{\Pi}_n = \boldsymbol{\Omega}(\alpha_i)\{-\boldsymbol{\Pi}_1 \sin\alpha_i + \boldsymbol{\Pi}_2 \cos\alpha_i\}^T \tag{33}$$

where $\Omega(\alpha_i)$ has been defined in eqn (3.174) of Ref.[11].

Using eqn (33) we can evaluate the SED intensity factors by the following definition

$$\mathbf{K}(c) = \{K_{II}\ K_I\ K_{III}\ K_D\}^T = \lim_{r\to 0}\sqrt{2\pi r}\,\mathbf{\Pi}_n(r)\,. \tag{34}$$

4 Application of BEM to determine SED intensity factors

In practical computations, one may evaluate the SED intensity factors in several ways such as extrapolation formulae, traction formulae, *J*-integral formulae [14], least-square method [15,16], and others [14]. In our analysis, the method of least-square is used, since only the EDEP field obtained from the BEM is required in the procedure. It therefore does not require much computer time for the *K*-factors calculation. Moreover, it is very easy to implement the method into our BEM computer program. That is why we select the least-square method, rather than another, to calculate SED intensity factors.

4.1 Relation between SED function and SED intensity factors

In order to take into account the crack-tip singularity of the SED field we choose the mapping function [17]

$$z_k - z_{k0} = w(\xi_k) = \xi_k^2\,, \qquad (k=1, 2, 3, 4, t) \tag{35}$$

where z_{k0} is the coordinate of the crack tip under consideration. Recall that the general expressions for the EDEP field and SED function of a linear thermopiezoelectric solid are [6, 7]

$$\begin{aligned} \mathbf{U} &= 2\,\mathrm{Re}[\mathbf{A}\mathbf{f}(\mathbf{z}) + \mathbf{c}g(z_t)], \\ \boldsymbol{\varphi} &= 2\,\mathrm{Re}[\mathbf{B}\mathbf{f}(\mathbf{z}) + \mathbf{d}g(z_t)]. \end{aligned} \tag{36}$$

The EDEP and SED fields in ξ-plane can then be written as

$$\begin{aligned} \mathbf{U} &= 2\,\mathrm{Re}[\mathbf{A}\mathbf{f}(\xi) + \mathbf{c}g(\xi_t)], \\ \Pi_2 &= 2\,\mathrm{Re}[\mathbf{B}\mathbf{f}'(\xi)/\xi + \mathbf{d}g'(\xi_t)/\xi_t]. \end{aligned} \tag{37}$$

With the usual definition, the vector of SED intensity factor, **K,** is evaluated by

$$\mathbf{K} = \lim_{\boldsymbol{\xi}\to 0}\boldsymbol{\xi}\sqrt{2\pi}\mathbf{\Pi}_2 = 2\sqrt{2\pi}\lim_{\boldsymbol{\xi}\to 0}\mathrm{Re}[\mathbf{B}\mathbf{f}'(\boldsymbol{\xi}) + \mathbf{d}g'(\xi_t)]\,. \tag{38}$$

The functions **f** and *g* near the crack tip can be assumed as simple polynomials of $\boldsymbol{\xi}$

$$\mathbf{f}(\boldsymbol{\xi}) \approx \sum_{j=1}^{2n}(\mathbf{s}_j + i\mathbf{s}_{2n+j})\boldsymbol{\xi}^j\,, \quad g(\xi_t) \approx \sum_{j=1}^{2n} r_j \xi_t^j \tag{39}$$

where r_j (j=1, 2, 3,…, 2n) are known complex constants, and $\mathbf{s}_j$ are real constant vectors to be determined.

On the crack surface which is traction-charge free, i.e., $\boldsymbol{\varphi}$=0, the substitution of eqn (39) into eqn $(36)_2$ yields

$$\boldsymbol{\varphi} = 2\,\mathrm{Re}\sum_{j=1}^{2n}[\mathbf{B}(\mathbf{s}_j + i\mathbf{s}_{2n+j})\boldsymbol{\xi}^j + \mathbf{d}r_j\xi_t^j] = 0\,. \tag{40}$$

Noting that $\boldsymbol{\xi}^j = \xi_t^j = (-x)^{j/2}$ along the crack surface, where x is the distance from crack tip to the point concerned, we have

$$\mathbf{s}_{2n+j} = \mathbf{B}_R^{-1}[-\mathbf{B}_I\mathbf{s}_j + \mathrm{Im}\{\mathbf{d}r_j\}], \qquad \text{for } j=1, 3, 5, \ldots, 2n\text{-}1, \tag{41}$$

$$\mathbf{s}_{2n+j} = \mathbf{B}_I^{-1}[\mathbf{B}_R\mathbf{s}_j + \mathrm{Re}\{\mathbf{d}r_j\}], \qquad \text{for } j=2, 4, 6, \ldots, 2n, \tag{42}$$

in which $\mathbf{B}_R$=Re(**B**), $\mathbf{B}_I$=Im(**B**).

Substituting eqns (41) and (42) into eqn (39), and then into eqns (37) and (38), yields

$$\begin{aligned}\mathbf{U} &= \sum_{j=1}^{2n}[\mathbf{Q}_j(\xi)\mathbf{s}_j + \mathbf{S}_j(\xi,\xi_t)],\\ \mathbf{K} &= 2\sqrt{2\pi}\,\mathrm{Re}[\mathbf{B}(\mathbf{I} - i\mathbf{B}_R^{-1}\mathbf{B}_I)\mathbf{s}_1 + i\mathbf{B}\mathbf{B}_R^{-1}\,\mathrm{Im}(\mathbf{d}r_1) + \mathbf{d}r_1],\end{aligned} \tag{43}$$

where

$$\mathbf{Q}_j(\xi) = [\mathbf{I} - i\mathbf{B}_R^{-1}\mathbf{B}_I]\xi^j,\ \mathbf{S}_j(\xi,\xi_t) = i\mathbf{B}_R^{-1}\mathrm{Im}[\mathbf{d}r_j]\xi^j + \mathbf{d}r_j\xi_t^j,\ (\,j = 1, 3, \ldots, 2n-1), \tag{44}$$

$$\mathbf{Q}_j(\xi) = [\mathbf{I} + i\mathbf{B}_I^{-1}\mathbf{B}_R]\xi^j,\ \mathbf{S}_j(\xi,\xi_t) = i\mathbf{B}_I^{-1}\mathrm{Re}[\mathbf{d}r_j]\xi^j + \mathbf{d}r_j\xi_t^j,\ (\,j = 2, 4, \ldots, 2n). \tag{45}$$

4.2 Simulating K by BEM and least-square method

The least-square method may be developed by considering the residual vector for EDEP field at point k (k=1, 2, …, m)

$$\mathbf{R}_k = \sum_{j=1}^{2n}[\mathbf{Q}_j(\boldsymbol{\xi}_k)\mathbf{s}_j + \mathbf{S}_j(\boldsymbol{\xi}_k, \xi_{tk})] - \mathbf{U}_k\,, \qquad (k=1, 2, \ldots, m) \tag{46}$$

where $\mathbf{U}_k$ is the EDEP vector at point k obtained from the BEM given in the previous section.

The minimum for the sum of the squares of the residual vector

$$\pi = \{\mathbf{s}\}^T[\mathbf{Q}]^T[\mathbf{Q}]\{\mathbf{s}\} - 2\{\mathbf{s}\}^T[\mathbf{Q}]^T(\{\mathbf{U}\} - \{\mathbf{S}\}) + \text{terms without } \{\mathbf{s}\} \tag{47}$$

provides

$$[\mathbf{Q}]^T[\mathbf{Q}]\{\mathbf{s}\} = [\mathbf{Q}]^T(\{\mathbf{U}\} - \{\mathbf{S}\})\,, \tag{48}$$

where

$$\{\mathbf{s}\} = \{\mathbf{s}_1, \mathbf{s}_2, \ldots, \mathbf{s}_{2n}\}^T, \quad \{\mathbf{U}\} = \{\mathbf{U}_1, \mathbf{U}_2, \ldots, \mathbf{U}_m\}^T, \tag{49}$$

$$\{\mathbf{S}\} = \{\mathbf{S}_1^*, \mathbf{S}_2^*, \ldots, \mathbf{S}_m^*\}^T, \quad \mathbf{S}_k^* = \sum_{j=1}^{2n}\mathbf{S}_j(\boldsymbol{\xi}_k, \xi_{tk})\,, \tag{50}$$

$$[\mathbf{Q}] = \begin{bmatrix} \mathbf{Q}_{11} & \mathbf{Q}_{21} & \cdots & \mathbf{Q}_{2n,1} \\ \mathbf{Q}_{12} & \mathbf{Q}_{22} & \cdots & \mathbf{Q}_{2n,2} \\ \cdots & \cdots & \cdots & \cdots \\ \mathbf{Q}_{1m} & \mathbf{Q}_{2m} & \cdots & \mathbf{Q}_{2n,m} \end{bmatrix}, \tag{51}$$

$$\mathbf{Q}_{jk} = \mathbf{Q}_j(\boldsymbol{\xi}_k) . \tag{52}$$

Once the unknown vector $\{\mathbf{s}\}$ has been obtained from eqn (48), the SED intensity factors $\mathbf{K}$ can be evaluated from eqn $(43)_2$. In the calculation, an appropriate number m can be set to obtain the required accuracy.

5 Numerical results

As an illustration, the proposed boundary element model is applied to the following two numerical examples in which an inclusion and a crack are involved. In all the calculations, the materials for the matrix and the elliptic inclusion are assumed to be $BaTiO_3$ and Cadmium Selenide, respectively. The material constants for the two materials are as follows:

(1) Material constants for $BaTiO_3$

$c_{11} = 150\,\text{GPa},\ c_{12} = 66\,\text{GPa},\ c_{13} = 66\,\text{GPa},\ c_{33} = 146\,\text{GPa},\ c_{44} = 44\,\text{GPa},$

$\alpha_{11} = 8.53\times10^{-6}\,\text{K}^{-1},\ \alpha_{33} = 1.99\times10^{-6}\,\text{K}^{-1},\ \lambda_3 = 0.133\times10^{5}\ \text{N/CK},$

$e_{31} = -4.35\,\text{C/m}^2,\ e_{33} = 17.5\,\text{C/m}^2,\ e_{15} = 11.4\,\text{C/m}^2,\ \kappa_{11} = 1115\,\kappa_0,$

$\kappa_{33} = 1260\,\kappa_0, \kappa_0 = 8.85\times10^{-12}\ \text{C}^2/\text{Nm}^2 = \text{Permittivity of free space}$

(2) Material constants for Cadmium Selenide

$c_{11} = 74.1\,\text{GPa},\ c_{12} = 45.2\,\text{GPa},\ c_{13} = 39.3\,\text{GPa},\ c_{33} = 83.6\,\text{GPa},$

$c_{44} = 13.2\,\text{GPa},\ \gamma_{11} = 0.621\times10^{6}\ \text{NK}^{-1}\text{m}^{-2},\quad \gamma_{33} = 0.551\times10^{6}\ \text{NK}^{-1}\text{m}^{-2},$

$g_3 = -0.294\times10^{5}\ \text{CK}^{-1}\text{m}^{-2},\quad e_{31} = -0.160\,\text{Cm}^{-2},\quad e_{33} = 0.347\,\text{Cm}^{-2},$

$e_{15} = 0.138\,\text{Cm}^{-2},\ \kappa_{11} = 82.6\times10^{-12}\ \text{C}^2\text{N}^{-1}\text{m}^{-2},\ \kappa_{33} = 90.3\times10^{-12}\ \text{C}^2\text{N}^{-1}\text{m}^{-2}.$

where c_{ij} is elastic stiffness, α_{11} and α_{33} are thermal expansion constants, λ_3 and g_3 are pyroelectric constants, e_{ij} is piezoelectric constants, γ_{ij} is piezothermal constant.

Since the values of the coefficient of heat conduction for $BaTiO_3$ and Cadmium Selenide could not be found in the literature, the values $k_{33}/k_{11}=1.5$ for $BaTiO_3$ and $k_{33}/k_{11}=1.8$ for Cadmium Selenide, $k_{13}=0$ and $k_{11}=1$ W/mK are assumed.

In our analysis, plane strain deformation is assumed and the crack line is assumed to be in the x_1-x_2 plane, i.e., $D_3=u_3=0$. Therefore the stress intensity factor vector $\mathbf{K}^*$ now has only three components (K_I, K_{II}, K_D).

In the least-square method, the SED intensity factors are affected by the parameters

n, d_{max} and d_{min}, where n is the number of terms in eqn (46), d_{max} is the maximum distance from crack tip to the n-point at which the residual vectors are calculated, and d_{min} is the minimum distance. In our analysis d_{min} is set to be $0.05c$.

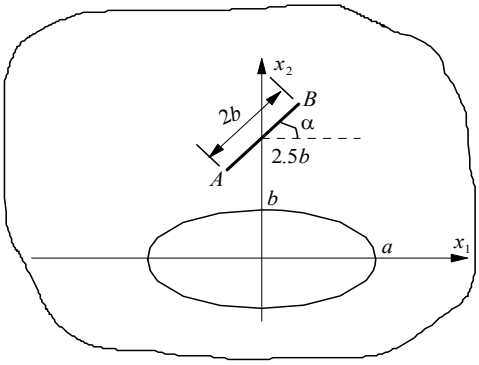

Fig. 2: Geometry of the crack-inclusion system.

Example 1: Consider a crack of length $2b$ and an inclusion embedded in an infinite plate as shown in Fig. 2. The uniform heat flow h_{n0} is applied on the crack face only. In our analysis, the crack was modelled by 40 linear elements. Table 1 shows that the numerical results for the coefficients of stress intensity factors β_i at point A (see Fig. 2) vary with d_{max} when the crack angle $\alpha = 0^\circ$ and n=5, 10, 15, respectively, where β_i are defined by

$$K_I = h_{n0} c\sqrt{\pi c}\gamma_{33}\beta_1 / k_1 ,$$
$$K_{II} = h_{n0} c\sqrt{\pi c}\gamma_{11}\beta_2 / k_1 , \tag{53}$$
$$K_D = h_{n0} c\sqrt{\pi c}\chi_3\beta_D / k_1 .$$

Table 1 The BEM results for coefficients β_i vs d_{max} in Example 1

d_{max}/c	n	β_1	β_2	β_D
0.5	5	1.230	0.328	0.755
	10	1.224	0.323	0.747
	15	1.222	0.322	0.745
1.0	5	1.225	0.321	0.749
	10	1.221	0.318	0.745
	15	1.220	0.318	0.743
1.5	5	1.231	0.328	0.757
	10	1.227	0.324	0.752
	15	1.226	0.323	0.750
SIEM		1.207	0.311	0.732

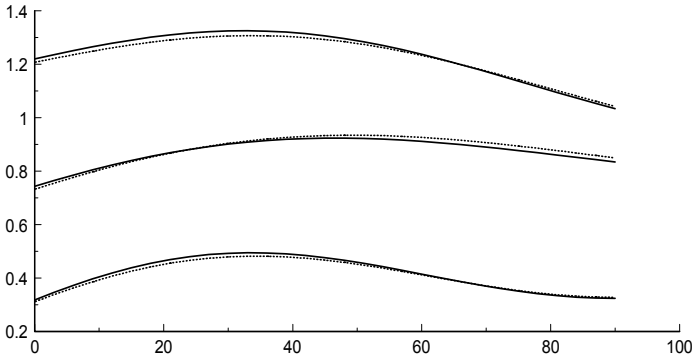

Fig. 3: The coefficients β_i versus crack angle α.

For comparison, the singular integral equation method (SIEM) given in [6,7] was used to obtain corresponding results. It can be seen from Table 1 that the results obtained using $d_{max}=c$ are often closer to those obtained by SIEM than by using $d_{max}=0.5c$ or $d_{max}=1.5c$. This is because more data can be included into the least-square method for a large d_{max}, but too large d_{max} may not represent the crack-tip properties and cause errors.

Figure 3 shows the results of coefficients β_i as a function of crack angle α when $d_{max}=c$ and n=15. It is evident from the figure that all the coefficients β_i are not very sensitive to the crack angle, but vary slightly with it. It is also evident that the two numerical models (BEM and SIEM) provide almost the same results.

Example 2: Consider a rectangular thermopiezoelectric plate containing a crack and an inclusion as shown in Fig. 4. In the calculation, each side of the outer boundary is modelled by 50 linear elements and the crack is divided into 40 linear elements, $d_{max}=b$ and n=15 are used. In Fig. 5 the coefficients of SED intensity factors β_i at point A (see Fig. 4) are presented as a function of crack orientation angle α. However, numerical results for such a problem are not yet available in the literature. For comparison, the well-known finite element method [18] is used to obtain corresponding results. In the calculation, an eight-node quadrilateral element model has been used. In addition, the three nodes along one of the sides of each of the quadrilateral elements are collapsed at the crack tip and the two adjoining mid-points are moved to the quarter distances [19], in order to produce $1/r^{1/2}$ type of singularity. It can be seen from Fig. 5 that the values of β_i are more sensitive to crack orientation than those in Example 1. They reach their peak values at $\alpha = 37^\circ$ for β_1, $\alpha = 42^\circ$ for β_2

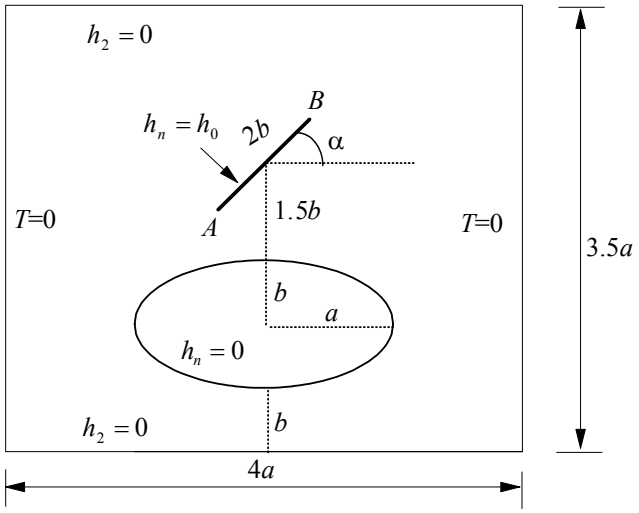

Fig. 4: Configuration of the crack-inclusion system in Example 2 (a=2b).

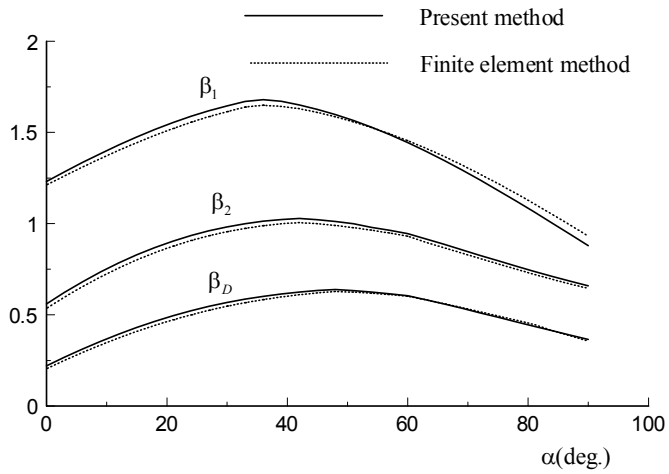

Fig. 5: SED intensity factors versus crack angle α.

and $\alpha = 50^\circ$ for β_D, respectively. It is also evident from Fig. 5 that the maximum discrepancy between the numerical results obtained from the two models is less than 5%.

5 Conclusion

Applications of boundary method to thermopiezoelectric materials with defects are discussed in this paper. A unified formulation for cracked half-plane, bimaterial, hole and inclusion problems of piezoelectricity has been presented. The study indicates that the formulation is applicable to multiple crack problems in both finite and infinite solids. Numerical results obtained from the present boundary element formulation and finite element approach are compared and they are in good agreement, but the former with less degree of freedom.

References

1. Lee JS and Jiang LZ. A boundary integral formulation and 2D fundamental solution for piezoelectric media. *Mech. Res. Comm*. 1994;21:47-54.
2. Lu P and Mahrenholtz O. A variational boundary element formulation for piezoelectricity. *Mech. Res. Comm*. 1994;21:605-611.
3. Ding HJ, Wang GP, and Chen WQ. Boundary integral formulation and 2D fundamental solutions for piezoelectric media. *Comp. Meth. Appl. Mech. Eng*. 1998;158:65-80.
4. Rajapakse RK. Boundary element methods for piezoelectric solids. *Proceedings of SPIE, Mathematics and Control in Smart Structures*, 1997;3039:418-428.
5. Xu XL and Rajapakse RK. Boundary element analysis of piezoelectric solids with defects. *Composites Part B: Engineering* 1998;29:655-669.
6. Hill LR and Farris TN. Three dimensional piezoelectric boundary elements. *Proceedings of SPIE, Mathematics and Control in Smart Structures* 1997;3039: 406-417.
7. Khutoryaansky N, Sosa H, and Zu WH. Approximate Green's functions and a boundary element method for electroelastic analysis of active materials. *Compu. & Struct*. 1998;66:289-299.
8. Qin QH. Thermoelectroelastic analysis of cracks in piezoelectric half-plane by BEM. *Computa. Mech*. 1999;23:353-360.
9. Qin QH and Lu M. BEM for crack-inclusion problems of plane thermo-piezoelectric solids. *Int. J. Numer. Meth. Eng*. 2000;48:1071-1088.
10. Liu YJ and Fan H. Analysis of thin piezoelectric solids by the boundary element method. *Comp. Meth. Appl. Mech. Eng*. 2002;191:2297-2315.
11. Qin QH. *Fracture Mechanics of Piezoelectric Materials*. Chapter 6, WIT Press, Southampton, 2001.
12. Qin QH and Mai YW. BEM for crack-hole problems in thermopiezoelectric materials. *Engineering Fracture Mechanics* 2002;69:577-588.
13. Yin HP and Ehrlacher A. Variational approach of displacement discontinuity method and application to crack problems. *Int. J. Fracture* 1993;63:135-153.
14. Aliabadi MH and Rooke DP. *Numerical Fracture Mechanics*. Computational Mechanics Publications: Southampton, 1991.
15. Ju SH. Simulating stress intensity factors for anisotropic materials by the least-square method. *Int. J. Frac*. 1996;81:283-397.

16. Ju SH. Simulating three-dimensional stress intensity factors by the least-square method. *Int. J. Numer. Meth. Eng*. 1998;43:1437-1451.
17. Khalil SA, Sun CT, and Kwang WC. Application of a hybrid finite element method to determine stress intensity factors in unidirectional composites. *Int. J. Frac*. 1986;31:37-51.
18. Oden, JT and Kelley BE. Finite element formulation of general electrothermo-elasticity problems. *Int. J. Numer. Meth. Eng*. 1971;3:161-179.
19. Anderson JL. *Fracture Mechanics: Fundamentals and Applications*. CRC Press: Boston, 1991.
20. Qin QH, General solutions for thermopiezoelectrics with various holes under thermal loading. 2000;37:5561-5578

Appendix A: Expressions for $a_m(z_t)$ (or $a_m(\zeta_t)$)

The function $a_m(z_t)$ has different form for different problem. For example,

$$a_m(z_t)=\frac{1}{2\pi}\int_{l_{m-1}}\{\ln(z_t-z_{t0}^{m-1})+b_1\ln(z_t-\bar{z}_{t0}^{m-1})\}\frac{l_{m-1}+s}{l_{m-1}}ds$$
$$+\frac{1}{2\pi}\int_{l_m}\{\ln(z_t-z_{t0}^{m})+b_1\ln(z_t-\bar{z}_{t0}^{m})\}\frac{l_m-s}{l_m}ds \tag{A1}$$

for bimaterial problems,

$$a_m(\zeta_t)=\frac{1}{2\pi}\int_{l_{m-1}}\left\{\ln(\zeta_t-\zeta_{t0}^{m-1})+\ln(\zeta_t^{-1}-\bar{\zeta}_{t0}^{m-1})+\sum_{j=1}^{\infty}(\Gamma_j^* c_j-\bar{c}_j)\zeta_t^{-j}\right\}\frac{l_{m-1}+s}{l_{m-1}}ds$$
$$+\frac{1}{2\pi}\int_{l_m}\left\{\ln(\zeta_t-\zeta_{t0}^{m})+\ln(\zeta_t^{-1}-\bar{\zeta}_{t0}^{m})+\sum_{j=1}^{\infty}(\Gamma_j^* c_j-\bar{c}_j)\zeta_t^{-j}\right\}\frac{l_m-s}{l_m}ds \tag{A2}$$

for a plate containing an elliptic inclusion and multiple cracks outside the inclusion, in which

$$\zeta_t=f(z_t)=\frac{z_t+\sqrt{z_t^2-a^2-p_1^{*2}b^2}}{a-ip_1^{*2}b},\quad \zeta_{t0}^{m-1}=f(z_{t0}^{m-1}),\ \ \zeta_{t0}^{m}=f(z_{t0}^{m}), \tag{A3}$$

and

$$a_m(z_t)=\frac{1}{2\pi}\int_{l_{m-1}}\{\ln(z_t-z_{t0}^{m-1})+\ln(z_t-\bar{z}_{t0}^{m-1})\}\frac{l_{m-1}+s}{l_{m-1}}ds$$
$$+\frac{1}{2\pi}\int_{l_m}\{\ln(z_t-z_{t0}^{m})+\ln(z_t-\bar{z}_{t0}^{m})\}\frac{l_m-s}{l_m}ds \tag{A4}$$

for the half-plane problem with multiple cracks, and

$$a_m(\zeta_t)=\frac{1}{2\pi}\int_{l_{m-1}}\{\ln(\zeta_t-\zeta_{t0}^{m-1})+\ln(\zeta_t^{-1}-\bar{\zeta}_{t0}^{m-1})\}\frac{l_{m-1}+s}{l_{m-1}}ds$$

$$+\frac{1}{2\pi}\int_{l_m}\{\ln(\zeta_t-\zeta_{t0}^m)+\ln(\zeta_t^{-1}-\overline{\zeta}_{t0}^m)\}\frac{l_m-s}{l_m}ds \tag{A5}$$

for a plate containing multiple cracks and a hole of various shapes, where ζ_t and ζ_{t0}^m are defined in [12,20].

In the formulations above z_{t0}^m is defined as

$$z_{t0}^{m-1}=d_{tm}+s(\cos\alpha_{m-1}+p_1^*\sin\alpha_{m-1}),\ z_{t0}^m=d_{tm}+s(\cos\alpha_m+p_1^*\sin\alpha_m) \tag{A6}$$

and $d_{tm}=x_{1m}+p_1^*x_{2m}$, (x_{1m},x_{2m}) represent the coordinates at node m, α_{m-1} is the angle between the element in the left of node m and the x_1-axis, with α_m defined similarly. It should be pointed out that the superscript "(1)" for variables ζ_t and z_t has been omitted in eqns (A1) and (A2) in order to simplify the writing.

Appendix B: Formulations of $\mathbf{u}_j$, $\mathbf{x}_j$ and $\mathbf{y}_j$

The expression of $\mathbf{u}_j$, $\mathbf{x}_j$ and $\mathbf{y}_j$ are presented for following four cases:

(i) a plate containing an elliptic inclusion and multiple cracks outside the inclusion

$$\mathbf{u}_j=\frac{1}{2\pi}\mathrm{Im}\int_{l_{j-1}}\left[\sum_{k=1}^{3}\mathbf{A}\left\langle f_{\alpha k}(\zeta_\alpha)\right\rangle\mathbf{q}_k+\sum_{k=4}^{5}\mathbf{A}\mathbf{f}_k(\boldsymbol{\zeta}_i)+\mathbf{c}g(\zeta_t)\right]\frac{l_{j-1}+s}{l_{j-1}}ds$$
$$+\frac{1}{2\pi}\mathrm{Im}\int_{l_j}\left[\sum_{k=1}^{5}\mathbf{A}\left\langle f_{\alpha k}(\zeta_\alpha)\right\rangle\mathbf{q}_k+\sum_{k=4}^{5}\mathbf{A}\mathbf{f}_k(\boldsymbol{\zeta}_i)+\mathbf{c}g(\zeta_t)\right]\frac{l_j-s}{l_j}ds, \tag{B1}$$

$$\mathbf{x}_j=-\frac{1}{2\pi}\mathrm{Im}\int_{l_{j-1}}\left[\sum_{k=1}^{3}\mathbf{A}\left\langle p_\alpha f'_{\alpha k}(\zeta_\alpha)\frac{\partial\zeta_\alpha}{\partial z_\alpha}\right\rangle\mathbf{q}_k+\sum_{k=4}^{5}\mathbf{A}\mathbf{P}\mathbf{f}_k^*\right.$$
$$\left.+\mathbf{c}\tau g'(\zeta_t)\frac{\partial\zeta_t}{\partial z_t}\right]\frac{l_{j-1}+s}{l_{j-1}}ds-\frac{1}{2\pi}\mathrm{Im}\{\int_{l_j}\left[\sum_{k=1}^{5}\mathbf{A}\left\langle p_\alpha f'_{\alpha k}(\zeta_\alpha)\frac{\partial\zeta_\alpha}{\partial z_\alpha}\right\rangle\mathbf{q}_k\right.$$
$$\left.+\sum_{k=4}^{5}\mathbf{A}\mathbf{P}\mathbf{f}_k^*+\mathbf{c}\tau g'(\zeta_t)\frac{\partial\zeta_t}{\partial z_t}\right]\frac{l_j-s}{l_j}ds, \tag{B2}$$

$$\mathbf{y}_j=\frac{1}{2\pi}\mathrm{Im}\int_{l_{j-1}}\left[\sum_{k=1}^{3}\mathbf{A}\left\langle f'_{\alpha k}(\zeta_\alpha)\frac{\partial\zeta_\alpha}{\partial z_\alpha}\right\rangle\mathbf{q}_k+\sum_{k=4}^{5}\mathbf{A}\mathbf{f}_k^*\right.$$
$$\left.+\mathbf{c}g'(\zeta_t)\frac{\partial\zeta_t}{\partial z_t}\right]\frac{l_{j-1}+s}{l_{j-1}}ds+\frac{1}{2\pi}\mathrm{Im}\int_{l_j}\left[\sum_{k=1}^{5}\mathbf{A}\left\langle f'_{\alpha k}(\zeta_\alpha)\frac{\partial\zeta_\alpha}{\partial z_\alpha}\right\rangle\mathbf{q}_k\right.$$
$$\left.+\sum_{k=4}^{5}\mathbf{A}\mathbf{f}_k^*+\mathbf{c}g'(\zeta_t)\frac{\partial\zeta_t}{\partial z_t}\right]\frac{l_j-s}{l_j}ds \tag{B3}$$

where

$$\mathbf{f}_4^* = \sum_{j=1}^{\infty} \left\langle j\zeta_\alpha^{j-1} \frac{\partial \zeta_\alpha}{\partial z_\alpha} \right\rangle \mathbf{e}_k \,, \tag{B4}$$

$$\mathbf{f}_5^* = \sum_{j=1}^{\infty} \left\langle -j\zeta_\alpha^{-j-1} \frac{\partial \zeta_\alpha}{\partial z_\alpha} \right\rangle \mathbf{t}_k \,. \tag{B5}$$

(ii) bimaterial problems

$$\mathbf{u}_j = \frac{1}{2\pi} \mathrm{Im} \int_{l_{j-1}} \{\mathbf{A}\left\langle f(y_1^{*(1)})\right\rangle \mathbf{q}_1 + \mathbf{c}[f(y_1^{(1)}) + b_1 f(y_2^{(1)})]\} \frac{l_{j-1}+s}{l_{j-1}} ds$$

$$+ \frac{1}{2\pi} \mathrm{Im} \int_{l_j} \{\mathbf{A}\left\langle f(y_1^{*(1)})\right\rangle \mathbf{q}_1 + \mathbf{c}[f(y_1^{(1)}) + b_1 f(y_2^{(1)})]\} \frac{l_j - s}{l_j} ds, \tag{B6}$$

$$\mathbf{x}_j = -\frac{1}{2\pi} \mathrm{Im} \int_{l_{j-1}} \{\mathbf{B}\left\langle p_k f'(y_1^{*(1)})\right\rangle \mathbf{q}_1 + \mathbf{d}p_1^* [f'(y_1^{(1)}) + b_1 f'(y_2^{(1)})]\} \frac{l_{j-1}+s}{l_{j-1}} ds$$

$$- \frac{1}{2\pi} \mathrm{Im} \int_{l_j} \{\mathbf{B}\left\langle p_k f'(y_1^{*(1)})\right\rangle \mathbf{q}_1 + \mathbf{d}p_1^* [f'(y_1^{(1)}) + b_1 f'(y_2^{(1)})]\} \frac{l_j - s}{l_j} ds, \tag{B7}$$

$$\mathbf{y}_j = \frac{1}{2\pi} \mathrm{Im} \int_{l_{j-1}} \{\mathbf{B}\left\langle f'(y_1^{*(1)})\right\rangle \mathbf{q}_1 + \mathbf{d}[f'(y_1^{(1)}) + b_1 f'(y_2^{(1)})]\} \frac{l_{j-1}+s}{l_{j-1}} ds$$

$$+ \frac{1}{2\pi} \mathrm{Im} \int_{l_j} \{\mathbf{B}\left\langle f'(y_1^{*(1)})\right\rangle \mathbf{q}_1 + \mathbf{d}[f'(y_1^{(1)}) + b_1 f'(y_2^{(1)})]\} \frac{l_j - s}{l_j} ds. \tag{B8}$$

(iii) half-plane problem with multiple cracks

$$\mathbf{u}_j = \frac{1}{2\pi} \mathrm{Im} \int_{l_{j-1}} [\mathbf{A}\left\langle f_*(z_\alpha)\right\rangle (-\mathbf{B}^{-1}\mathbf{d}) + \mathbf{c}f_*(z_t)] \frac{l_{j-1}+s}{l_{j-1}} ds$$

$$+ \frac{1}{2\pi} \mathrm{Im} \int_{l_j} [\mathbf{A}\left\langle f_*(z_k)\right\rangle (-\mathbf{B}^{-1}\mathbf{d}) + \mathbf{c}f_*(z_t)] \frac{l_j - s}{l_j} ds, \tag{B9}$$

$$\mathbf{x}_j = \frac{1}{2\pi} \mathrm{Im} \int_{l_{j-1}} [\mathbf{B}\left\langle p_\alpha f_*'(z_\alpha)\right\rangle (\mathbf{B}^{-1}\mathbf{d}) - \mathbf{d}p_1^* f_*'(z_t)] \frac{l_{j-1}+s}{l_{j-1}} ds$$

$$+ \frac{1}{2\pi} \mathrm{Im} \int_{l_j} [\mathbf{B}\left\langle p_\alpha f_*'(z_\alpha)\right\rangle (\mathbf{B}^{-1}\mathbf{d}) - \mathbf{d}p_1^* f_*'(z_t)] \frac{l_j - s}{l_j} ds, \tag{B10}$$

$$\mathbf{y}_j = -\frac{1}{2\pi} \mathrm{Im} \int_{l_{j-1}} [\mathbf{B}\left\langle f_*'(z_\alpha)\right\rangle (\mathbf{B}^{-1}\mathbf{d}) - \mathbf{d}f_*'(z_t)] \frac{l_{j-1}+s}{l_{j-1}} ds$$

$$- \frac{1}{2\pi} \mathrm{Im} \int_{l_j} [\mathbf{B}\left\langle f_*'(z_\alpha)\right\rangle (\mathbf{B}^{-1}\mathbf{d}) - \mathbf{d}f_*'(z_t)] \frac{l_j - s}{l_j} ds, \tag{B11}$$

where

$$f_*(z_x) = (z_x - z_{t0})[\ln(z_x - z_{t0}) - 1] - (z_x - \bar{z}_{t0})[\ln(z_x - \bar{z}_{t0}) - 1] \,. \tag{B12}$$

(iv) a plate containing multiple cracks and a hole of various shapes

$$\mathbf{u}_j = -\frac{1}{2\pi}\mathrm{Im}\int_{l_{j-1}} [\mathbf{A}(\mathbf{f}_1(\mathbf{z}) + \mathbf{f}_2(\mathbf{z})\mathbf{P}^{-1}\overline{\tau})\mathbf{B}^{-1}\overline{\mathbf{d}} - \mathbf{c}g(z_t)]\frac{l_{j-1}+s}{l_{j-1}}ds$$
$$-\frac{1}{2\pi}\mathrm{Im}\int_{l_j} [\mathbf{A}(\mathbf{f}_1(\mathbf{z}) + \mathbf{f}_2(\mathbf{z})\mathbf{P}^{-1}\overline{\tau})\mathbf{B}^{-1}\overline{\mathbf{d}} - \mathbf{c}g(z_t)]\frac{l_j - s}{l_j}ds, \tag{B13}$$

$$\mathbf{x}_j = \frac{1}{2\pi}\mathrm{Im}\int_{l_{j-1}} [\mathbf{B}(\mathbf{f}_1'(\mathbf{z})\mathbf{P} + \mathbf{f}_2'(\mathbf{z})\overline{p}_1^*)\mathbf{B}^{-1}\overline{\mathbf{d}} - \mathbf{c}p_1^* g'(z_t)]\frac{l_{j-1}+s}{l_{j-1}}ds$$
$$+\frac{1}{2\pi}\mathrm{Im}\int_{l_j} [\mathbf{B}(\mathbf{f}_1'(\mathbf{z})\mathbf{P} + \mathbf{f}_2'(\mathbf{z})\overline{p}_1^*)\mathbf{B}^{-1}\overline{\mathbf{d}} - \mathbf{c}p_1^* g'(z_t)]\frac{l_j - s}{l_j}ds, \tag{B14}$$

$$\mathbf{y}_j = -\frac{1}{2\pi}\mathrm{Im}\int_{l_{j-1}} [\mathbf{B}(\mathbf{f}_1'(\mathbf{z}) + \mathbf{f}_2'(\mathbf{z}))\mathbf{B}^{-1}\overline{\mathbf{d}} - \mathbf{c}g'(z_t)]\frac{l_{j-1}+s}{l_{j-1}}ds$$
$$-\frac{1}{2\pi}\mathrm{Im}\int_{l_j} [\mathbf{B}(\mathbf{f}_1'(\mathbf{z}) + \mathbf{f}_2'(\mathbf{z}))\mathbf{B}^{-1}\overline{\mathbf{d}} - \mathbf{c}g'(z_t)]\frac{l_j - s}{l_j}ds. \tag{B15}$$

Thus, the SED and EDEP on a boundary induced by temperature discontinuity are of the form

$$\mathbf{t}_n^{\theta}(s) = \Pi_i n_i = \sum_{j=1}^{M} (\mathbf{x}_j n_1 + \mathbf{y}_j n_2)\hat{T}_j, \qquad \mathbf{U}_T^{\theta}(s) = \sum_{j=1}^{M} \mathbf{u}_j \hat{T}_j . \tag{B16}$$

In general, $\mathbf{t}_n^{\theta}(s) \neq 0$ over Γ_t (the boundary on which SED is prescribed) and $\mathbf{U}_T^{\theta}(s) \neq 0$ over Γ_u (the boundary on which EDEP is prescribed). To balance the SED and EDEP on the corresponding boundaries, we must superpose a solution of the corresponding isothermal problem with a SED vector (or a EDEP vector) equal and opposite to those of eqn (B16). The details are given in the sub-section 3.2.

Appendix C: Expressions of $\varphi(\mathbf{b})$ and $\mathbf{U}(\mathbf{b})$

(i) a plate containing a hole and a dislocation **b** outside the inclusion

$$\mathbf{U}(\mathbf{b}) = \frac{1}{\pi}\mathrm{Im}[\mathbf{A}\langle \ln(\zeta_\alpha - \zeta_{\alpha 0})\rangle \mathbf{B}^T]\mathbf{b} + \frac{1}{\pi}\sum_{\beta=1}^{4}\mathrm{Im}[\mathbf{A}\langle \ln(\zeta_\alpha - \overline{\zeta}_{\beta 0})\rangle \mathbf{B}^{-1}\overline{\mathbf{B}}\mathbf{I}_\beta\overline{\mathbf{B}}^T]\mathbf{b} \tag{C1}$$

$$\varphi(\mathbf{b}) = \frac{1}{\pi}\mathrm{Im}[\mathbf{B}\langle \ln(\zeta_\alpha - \zeta_{\alpha 0})\rangle \mathbf{B}^T]\mathbf{b} + \frac{1}{\pi}\sum_{\beta=1}^{4}\mathrm{Im}[\mathbf{B}\langle \ln(\zeta_\alpha - \overline{\zeta}_{\beta 0})\rangle \mathbf{B}^{-1}\overline{\mathbf{B}}\mathbf{I}_\beta\overline{\mathbf{B}}^T]\mathbf{b} \tag{C2}$$

where diag[$\delta_{1\beta}$, $\delta_{2\beta}$, $\delta_{3\beta}$, $\delta_{4\beta}$].

(ii) half-plane problems

$$\mathbf{U}(\mathbf{b}) = \frac{1}{\pi}\mathrm{Im}[\mathbf{A}\langle \ln(z_\alpha - z_{\alpha 0})\rangle \mathbf{B}^T]\mathbf{b} + \frac{1}{\pi}\sum_{\beta=1}^{4}\mathrm{Im}[\mathbf{A}\langle \ln(z_\alpha - \overline{z}_{\beta 0})\rangle \mathbf{B}^{-1}\overline{\mathbf{B}}\mathbf{I}_\beta\overline{\mathbf{B}}^T]\mathbf{b} \tag{C3}$$

$$\varphi(\mathbf{b}) = \frac{1}{\pi}\mathrm{Im}[\mathbf{B}\langle \ln(z_\alpha - z_{\alpha 0})\rangle \mathbf{B}^T]\mathbf{b} + \frac{1}{\pi}\sum_{\beta=1}^{4}\mathrm{Im}[\mathbf{B}\langle \ln(z_\alpha - \overline{z}_{\beta 0})\rangle \mathbf{B}^{-1}\overline{\mathbf{B}}\mathbf{I}_\beta\overline{\mathbf{B}}^T]\mathbf{b} \tag{C4}$$

(iii) biomaterial problems
For a bimaterial plate subjected to a line dislocation **b** located in the upper half-plane at $z_0(x_{10}, x_{20})$, the solution is given by[11]

$$\mathbf{U}^{(1)} = \frac{1}{\pi}\mathrm{Im}\{\mathbf{A}^{(1)}\left\langle \ln(z_\alpha^{(1)} - z_{\alpha 0}^{(1)})\right\rangle \mathbf{B}^T\}\mathbf{b} + \sum_{\beta=1}^{4}\frac{1}{\pi}\mathrm{Im}\{\mathbf{A}^{(1)}\left\langle \ln(z_\alpha^{(1)} - \bar{z}_{\beta 0}^{(1)})\right\rangle \mathbf{q}_\beta^{(1)}\}\,, \tag{C5}$$

$$\varphi^{(1)} = \frac{1}{\pi}\mathrm{Im}\{\mathbf{B}^{(1)}\left\langle \ln(z_\alpha^{(1)} - z_{\alpha 0}^{(1)})\right\rangle \mathbf{B}^T\}\mathbf{b} + \sum_{\beta=1}^{4}\frac{1}{\pi}\mathrm{Im}\{\mathbf{B}^{(1)}\left\langle \ln(z_\alpha^{(1)} - \bar{z}_{\beta 0}^{(1)})\right\rangle \mathbf{q}_\beta^{(1)}\} \tag{C6}$$

for material 1 in $x_2>0$ and

$$\mathbf{U}^{(2)} = \sum_{\beta=1}^{4}\frac{1}{\pi}\mathrm{Im}\{\mathbf{A}^{(2)}\left\langle \ln(z_\alpha^{(2)} - z_{\beta 0}^{(1)})\right\rangle \mathbf{q}_\beta^{(2)}\}\,, \tag{C7}$$

$$\boldsymbol{\varphi}^{(2)} = \sum_{\beta=1}^{4}\frac{1}{\pi}\mathrm{Im}\{\mathbf{B}^{(2)}\left\langle \ln(z_\alpha^{(2)} - z_{\beta 0}^{(1)})\right\rangle \mathbf{q}_\beta^{(2)}\} \tag{C8}$$

where

$$\mathbf{q}_\beta^{(1)} = \mathbf{B}^{(1)-1}[\mathbf{I} - 2(\mathbf{M}^{(1)-1} + \overline{\mathbf{M}}^{(2)-1})^{-1}\mathbf{L}^{(1)-1}]\overline{\mathbf{B}}^{(1)}\mathbf{I}_\beta\overline{\mathbf{B}}^T\mathbf{b}\,, \tag{C9}$$

$$\mathbf{q}_\beta^{(2)} = 2\mathbf{B}^{(2)-1}(\overline{\mathbf{M}}^{(1)-1} + \mathbf{M}^{(2)-1})^{-1}\mathbf{L}^{(1)-1}\mathbf{B}^{(1)}\mathbf{I}_\beta\mathbf{B}^T\mathbf{b}\,, \tag{C10}$$

with $\mathbf{M}^{(j)} = -i\mathbf{B}^{(j)}\mathbf{A}^{(j)-1}$ is the surface impedance matrix.

(iv) inclusion problems
For the case of a plate containing an elliptic inclusion and a dislocation outside the inclusion the expressions of $\varphi(\mathbf{b})$ and $\mathbf{U}(\mathbf{b})$ is too complex and we omit those details for conciseness, which can be found in [9,11].

Appendix D: Expressions of $\mathbf{D}_m(\zeta)$

(i) a plate containing an elliptic inclusion and multiple cracks outside the inclusion

$$\begin{aligned}\mathbf{D}_m(\boldsymbol{\zeta}) = \frac{1}{\pi}\int_{l_{m-1}} &\left\{\left\langle \ln(\zeta_\alpha - \zeta_{\alpha 0}^{m-1})\right\rangle \mathbf{B}^T + \sum_{k=1}^{\infty}\left\langle \zeta_\alpha^{-k}\right\rangle \mathbf{E}_k \right.\\ &\left. + \sum_{\beta=1}^{4}\left\langle \ln(\zeta_\alpha^{-1} - \overline{\zeta}_{\beta 0}^{m-1})\right\rangle \mathbf{B}^{-1}\overline{\mathbf{B}}\mathbf{I}_\beta\overline{\mathbf{B}}^T\right\}\frac{l_{m-1}-s}{l_{m-1}}ds\\ + \frac{1}{\pi}\int_{l_m} &\left\{\left\langle \ln(\zeta_\alpha - \zeta_{\alpha 0}^{m})\right\rangle \mathbf{B}^T + \sum_{k=1}^{\infty}\left\langle \zeta_\alpha^{-k}\right\rangle \mathbf{E}_k\right.\end{aligned}$$

$$+\sum_{\beta=1}^{4}\left\langle \ln(\zeta_\alpha^{-1}-\overline{\zeta}_{\beta 0}^{m})\right\rangle \mathbf{B}^{-1}\overline{\mathbf{B}}\mathbf{I}_\beta\overline{\mathbf{B}}^{T}\Bigg\}\frac{s}{l_m}ds \tag{D1}$$

in which ζ_α can be expressed in terms of s by the relations

$$\zeta_\alpha = f(z_\alpha)=\frac{z_\alpha+\sqrt{z_\alpha^2-a^2-p_\alpha^2b^2}}{a-ip_\alpha b},\qquad \zeta_{\alpha 0}^{m\text{-}1}=f(z_{\alpha 0}^{m-1}),\ \ \zeta_{\alpha 0}^{m}=f(z_{\alpha 0}^{m}),$$

$$z_{\alpha 0}^{m-1}=d_{\alpha m}+s(\cos\alpha_{m-1}+p_\alpha\sin\alpha_{m-1}),\ z_{\alpha 0}^{m}=d_{\alpha m}+s(\cos\alpha_{m}+p_\alpha\sin\alpha_{m}) \tag{D2}$$

and $d_{\alpha m}=x_{1m}+p_\alpha x_{2m}$.

(ii) half-plane problem with multiple cracks

$$\mathbf{D}_m(\mathbf{z})=\frac{1}{\pi}\int_{l_{m-1}}\left\{\left\langle \ln(z_{\alpha\alpha 0}^{m-1})\right\rangle\mathbf{B}^{T}+\sum_{\beta=1}^{4}\left\langle \ln(z_{\alpha\beta 0}^{m-1})\right\rangle\mathbf{B}^{-1}\overline{\mathbf{B}}\mathbf{I}_\beta\overline{\mathbf{B}}^{T}\right\}\frac{l_{m-1}+s}{l_{m-1}}ds$$
$$+\frac{1}{\pi}\int_{l_m}\left\{\left\langle \ln(z_{\alpha\alpha 0}^{m})\right\rangle\mathbf{B}^{T}+\sum_{\beta=1}^{4}\left\langle \ln(z_{\alpha\beta 0}^{m})\right\rangle\mathbf{B}^{-1}\overline{\mathbf{B}}\mathbf{I}_\beta\overline{\mathbf{B}}^{T}\right\}\frac{l_m-s}{l_m}ds. \tag{D3}$$

where $z_{\alpha\alpha 0}^{m}=z_\alpha-z_{\alpha 0}^{m}$ and $z_{\alpha\beta 0}^{m}=z_\alpha-\overline{z}_{\beta 0}^{m}$.

(iii) bimaterial problems

$$\mathbf{D}_m(\mathbf{z})=\frac{1}{\pi}\int_{l_{m-1}}\left\{\left\langle \ln(z_{\alpha\alpha 0}^{m-1})\right\rangle\mathbf{B}^{T}+\sum_{\beta=1}^{4}\left\langle \ln(z_{\alpha\beta 0}^{m-1})\right\rangle\mathbf{B}^{*}\overline{\mathbf{B}}\mathbf{I}_\beta\overline{\mathbf{B}}^{T}\right\}\frac{l_{m-1}+s}{l_{m-1}}ds$$
$$+\frac{1}{\pi}\int_{l_m}\left\{\left\langle \ln(z_{\alpha\alpha 0}^{m})\right\rangle\mathbf{B}^{T}+\sum_{\beta=1}^{4}\left\langle \ln(z_{\alpha\beta 0}^{m})\right\rangle\mathbf{B}^{*}\overline{\mathbf{B}}\mathbf{I}_\beta\overline{\mathbf{B}}^{T}\right\}\frac{l_m-s}{l_m}ds. \tag{D4}$$

(iv) a plate containing multiple cracks and a hole of various shapes (see Section 4.11 of Rref.[11])

$$\mathbf{D}_m(\boldsymbol{\zeta})=\frac{1}{\pi}\int_{l_{m-1}}\left\{\left\langle \ln(\zeta_\alpha-\zeta_{\alpha 0}^{m-1})\right\rangle\mathbf{B}^{T}+\sum_{\beta=1}^{4}\left\langle \ln(\zeta_\alpha^{-1}-\overline{\zeta}_{\beta 0}^{m-1})\right\rangle\mathbf{B}^{-1}\overline{\mathbf{B}}\mathbf{I}_\beta\overline{\mathbf{B}}^{T}\right\}\frac{l_{m-1}+s}{l_{m-1}}ds$$
$$+\frac{1}{\pi}\int_{l_m}\left\{\left\langle \ln(\zeta_\alpha-\zeta_{\alpha 0}^{m})\right\rangle\mathbf{B}^{T}+\sum_{\beta=1}^{4}\left\langle \ln(\zeta_\alpha^{-1}-\overline{\zeta}_{\beta 0}^{m})\right\rangle\mathbf{B}^{-1}\overline{\mathbf{B}}\mathbf{I}_\beta\overline{\mathbf{B}}^{T}\right\}\frac{l_m-s}{l_m}ds. \tag{D5}$$